Table 1 Axisymmetric static and dynamic buckling loads of shallow conical caps

λ	3	4	5	6	7	8	9	10	11	12	13	14
p_s	...	0.470	0.430	0.405	0.400	0.388	0.380	0.374	0.370	0.367	0.365	0.363
p_D	0.35 0.36	0.33	0.32	0.31	0.30 0.31	0.30 0.31	0.30	0.29 0.30	0.29	0.29	0.29	0.29

Table 2 Axisymmetric static and dynamic buckling loads of shallow spherical caps

λ	4	4.5	5	5.5	6	6.5	7	7.5	8	9	10	11	12	13	14	15
p_s Ref. 2	0.578	...	0.629	0.762 0.763	0.995	...	1.068	...	1.130	0.931 0.940	0.822 0.830	0.83 0.84	0.96 0.97	0.96 0.97	0.98 0.99	0.98 0.99
p_D Ref. 1	0.45	...	0.49	...	...	...	0.56	0.50	0.44	0.39	0.42	0.50	...	0.42	...	...
p_D present results	...	0.46	...	0.57	0.62	0.65	...	...	...	...	...	...	0.45	...	...	...

constructed are given in Table 1. In Table 1, p_s and p_D refer to the axisymmetric static and dynamic buckling loads, respectively.

The axisymmetric static and dynamic buckling curves for the clamped shallow spherical shell are shown in Fig. 2 and the corresponding numerical data are given in Table 2. The dashed curve of Fig. 2 is the axisymmetric dynamic buckling curve obtained by plotting the results obtained from Ref. 1, the numerical data of which is shown in Table 2. The dotted curve is a modification of the dashed curve arrived at by calculating the dynamic buckling loads for values of λ intermediate to those considered in Ref. 1 and using the same time response.

The striking similarity between the axisymmetric static and dynamic buckling curves for both the clamped shallow spherical and conical shells is apparent from an inspection of Figs. 1 and 2; the similarity being more pronounced for the conical shell. A very satisfactory empirical relation between the axisymmetric static and dynamic buckling loads for the clamped shallow conical shell for the range of λ considered in the present study is

$$(p_D)_\lambda = (p_s)_{\lambda+1.9} - 0.07 \tag{5}$$

Equation (5) implies that, if the axisymmetric dynamic buckling curve for the conical shell is translated 1.9 λ units to the right and 0.7 p units upward, then it will coincide closely with the corresponding axisymmetric static buckling curve. The maximum relative error between values of the dynamic buckling loads obtained from Eq. (5) and those shown in Table 1 is approximately 2%.

The similarity between the axisymmetric static and dynamic buckling curves for clamped shallow spherical shells is not as pronounced for the full range of λ considered, however, striking similarities exist for a significant range of λ. Figure 3 shows the axisymmetric static and dynamic buckling curves for the clamped shallow spherical shell where the dynamic buckling curve has been translated 1.4 λ units to the right and 4.8 p_s units upward. Inspection of these curves shows the similarity for the range $5.5 < \lambda < 11.5$ of the upper abscissa. The cross marks on the figure indicate the critical dynamic buckling loads obtained by Stephens and Fulton[3] using a larger response time. The reduction of the dynamic buckling loads, especially for $\lambda = 7.5$, 8, and 10 (upper abscissa), increases the similarity of the curves.

The conclusions suggested by this Note are: that there is a striking similarity between the axisymmetric static and dynamic buckling curves for both the clamped shallow spherical and conical shells; and if there exists a relationship between the axisymmetric static and dynamic buckling curves for these shells it must depend on λ. The fact that the uniform pressure of infinite duration shifts the dynamic buckling curve not only downward, as is expected because of the inertia force, but also to the left is noteworthy; the reasons for which are worth exploring.

References

[1] Huang, N. C., "Axisymmetric Dynamic Snap-Through of Elastic Clamped Shallow Spherical Shells," *AIAA Journal*, Vol. 7, No. 2, Feb. 1969, pp. 215–220.

[2] Huang, N. C., "Unsymmetrical Buckling of Thin Shallow Spherical Shells," *Journal of Applied Mechanics*, Vol. 31, Sept. 1964, p. 447.

[3] Stephens, W. B. and Fulton, R. E., "Axisymmetric Static and Dynamic Buckling of Spherical Caps Due to Centrally Distributed Pressures," *AIAA Journal*, Vol. 7, No. 11, Nov. 1969, p. 2120.

[4] Famili, J., "Asymmetric Buckling of Finitely Deformed Conical Shells," *AIAA Journal*, Vol. 3, No. 8, Aug. 1965, p. 1456.

Townsend Structure Parameters

R. S. Azad*

University of Manitoba, Winnipeg, Manitoba, Canada

Nomenclature

K_1, K_2 = Townsend's turbulence parameters [Eqs. (1) and (2)]
u,v,w = instantaneous values of velocity fluctuations in x,y, and z directions, respectively
x,y,z = distances in the axial, radial, and circumferential directions, respectively
$\langle\ \rangle$ = time average
$\langle q^2 \rangle$ = $\langle u^2 \rangle + \langle v^2 \rangle + \langle w^2 \rangle$
Re = Reynolds number based on diameter of pipe and mean velocity
δ^* = boundary-layer displacement thickness
θ = boundary-layer momentum thickness
δ^{**} = boundary-layer energy thickness

TOWNSEND[1] had defined two parameters; namely

$$K_1 = [\langle v^2 \rangle - \langle w^2 \rangle]/[\langle v^2 \rangle + \langle w^2 \rangle] \tag{1}$$

and

$$K_2 = [3\ \langle u^2 \rangle / \langle q^2 \rangle] - 1 \tag{2}$$

These parameters indicate the relative values of three intensities. Townsend[2] has also used these parameters to predict the equilibrium structure in fully strained turbulence. The author has adopted these parameters to investigate the structure of the diverging flow in a conical diffuser. The conical diffuser has an 8° solid angle, an area ratio of 4:1, and an inlet diameter of 10 cm. A pipe, 166 cm in length and

Received August 12, 1970; revision received September 17, 1970.

* Associate Professor, Department of Mechanical Engineering.

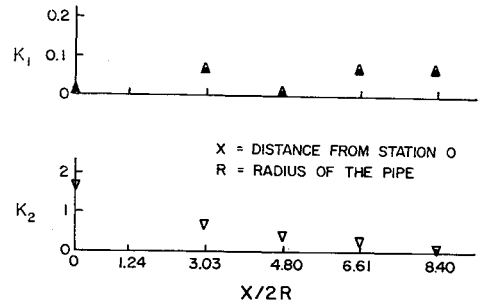

Fig. 1 Structure parameters on the center line.

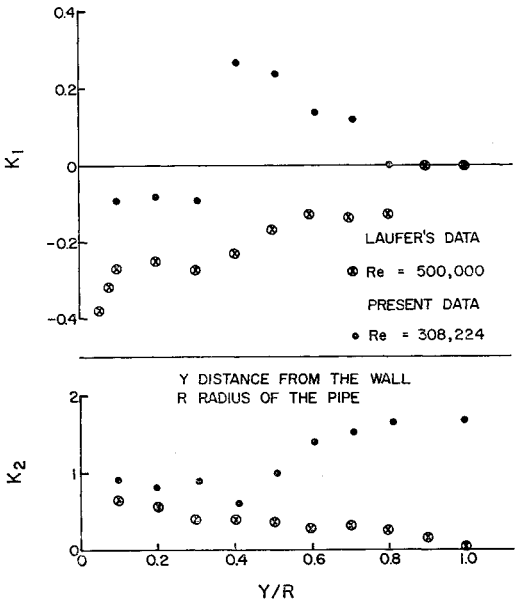

Fig. 2 Structure parameters at diffuser inlet.

10 cm in diameter was connected upstream of the diffuser to generate a boundary layer. Station 0 was located at 12.38 cm upstream of the diffuser, whereas stations 3, 6, 9, and 12 were at $\frac{1}{4}$, $\frac{1}{2}$, $\frac{3}{4}$, and 1 of the length of the diffuser, respectively. The inlet conditions to the diffuser were: Re = 308,224, δ^* = 0.3213 cm, θ = 0.2062 cm, and δ^{**} = 0.3764 cm. The measurements of turbulence were made by Disa equipment.

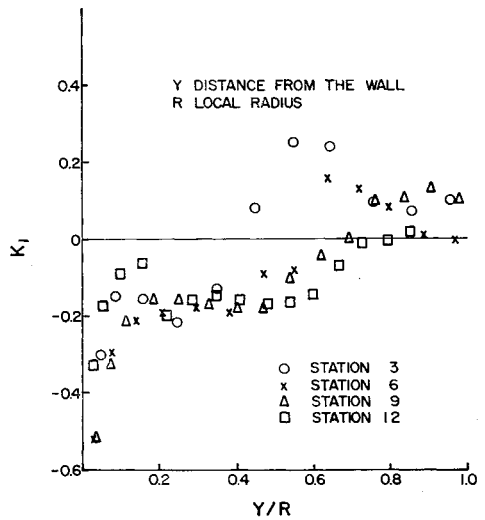

Fig. 3 Structure parameter K_1 in diffuser.

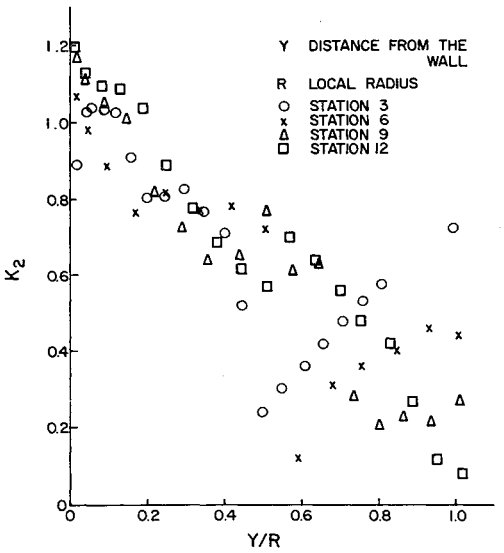

Fig. 4 Structure parameter K_2 in diffuser.

The variation of parameters K_1 and K_2 on the center line, and the lateral variations of these parameters at station 0 are shown in Fig. 1 and Fig. 2, respectively. Figure 2 also includes Laufer's results[3] in fully developed turbulent pipe flow for comparison. Figure 3 demonstrates the lateral variations of K_1, whereas Fig. 4 illustrates the lateral variations of K_2 at stations 3, 6, 9, and 12.

On the center line, K_1 has an average value of 0.03, i.e., approximately equals to zero and the value of K_2 tends to zero at the exit of the diffuser. This means that the general tendency of turbulence is towards isotropy as the flow proceeds to the outlet of the diffuser.

Figure 2 demonstrates the difference between developing flow and fully developed flow in pipes, since the present data were obtained in the developing flow. For the fully developed flow, K_1 has a negative value on major part of the radius of the pipe and attains the value of zero about the center of the pipe. In the case of developing flow in pipes, the parameter K_1 has a positive value for about 0.4 part of the radius. When the structure parameter K_2 in Fig. 2 is examined, K_2 decreases in the case of the fully developed pipe flow but increases in the case of developing flow as one goes from the wall to the center of the pipe. In conclusion, it seems the flow may be defined as fully developed if the parameter $K_1 \leqslant 0$ and the parameter K_2 decreases monotonically to zero at the center of the pipe.

The nature of the flow structure in the diffuser (Figs. 3 and 4) may also be decided on the same criteria as of the pipe flow. Examining Figs. 3 and 4, it is clear that the parameter K_1 is tending to the value $\leqslant 0$, and the parameter K_2 has the general tendency to decrease monotonically from the wall to the center of the diffuser. It seems the positive value of K_1 may be attributed to the mechanism of mixing in the flow, and its value is constant when the equilibrium of turbulent structure is attained in general. The structure parameter K_2 increases during the initial period after approximately half the local radius of the diffuser but decreases during the final period. The behaviour of K_2 may be the result of the rapid distortion. However, the general tendency of K_2 at stations 0, 3, and 6 is the same. This means that the general tendency of K_2 to increase after about half the local radius can only be attributed to the developing flow.

References

[1] Townsend, A. A., *The Structure of Turbulent Shear Flow*, 1st ed., Cambridge University Press, London, 1956, p. 74.

[2] Townsend, A. A., *The Structure of Turbulent Shear Flow*, 1st ed., Cambridge University Press, London, 1956, p. 76.

[3] Laufer, J., "The Structure of Turbulence in Fully Developed Pipe Flow," Rept. 1174, 1954, NACA.